

Giant cross-Kerr nonlinearity in carbon nanotube quantum dots with spin-orbit coupling

Hui Sun,^{1,2} Xun-Li Feng,^{1,2} Shangqing Gong,³ and C. H. Oh^{1,2}

¹*Department of Physics, National University of Singapore, 2 Science Drive 3, Singapore 117542, Singapore*

²*Centre for Quantum Technologies, National University of Singapore, 3 Science Drive 2, Singapore 117543, Singapore*

³*State Key Laboratory of High Field Laser Physics, Shanghai Institute of Optics and Fine Mechanics, Chinese Academy of Sciences, Shanghai 201800, China*

(Received 20 January 2009; revised manuscript received 16 April 2009; published 8 May 2009)

We investigate the nonlinear interaction between two weak optical fields in carbon nanotube quantum dots based on electromagnetically induced transparency and spin-orbit coupling. Our results show, owing to the energy differences produced by strong spin-orbit coupling, that a giant cross-Kerr nonlinearity can be achieved with group-velocity matching, while the probe- and signal-fields absorptions are suppressed simultaneously. We demonstrate that such enhanced nonlinear optical effects can be employed to implement controlled-phase gate between pairs of single-photon pulses with high fidelity and to generate entanglement of coherent Schrödinger-cat states.

DOI: [10.1103/PhysRevB.79.193404](https://doi.org/10.1103/PhysRevB.79.193404)

PACS number(s): 78.67.Ch, 42.65.-k, 78.67.Hc

Photons are good candidates for quantum bits because they do not interact strongly with their environment and can be transmitted over long distances. The strong nonlinear interaction between photons lie at the heart of quantum effects in optics such as frequency conversion,¹ the quantum entanglement of ultraslow photons² and ultraslow optical solitons,³ nonlinear phase gate,^{4,5} single-photon propagation controls,⁶ and so on. However, given the weakness of non-resonant optical nonlinearities and the dominant role of absorption in resonant process, the combination of a large nonlinear susceptibility and reduced—especially canceled—resonant absorption appears to be incompatible in conventional media. Electromagnetically induced transparency (EIT) (Ref. 7) technology is a promising avenue for solving this problem because it can modify the linear and nonlinear optical properties dramatically. Based on EIT and double EIT, some feasible schemes for achieving giant Kerr nonlinearity with reduced absorption have been studied theoretically^{4,5,8–10} and observed experimentally.^{11,12}

In comparison with atomic systems, the interaction between semiconducting quantum dots (QDs)/carbon nanotube (CNT) and optical fields is strongly enhanced due to the large dipole moments [$\sim 10^{-17}$ esu cm in QDs (Ref. 13) and $\sim 10^{-18}$ esu cm in CNT (Ref. 14)]. The QDs and CNT are thereby regarded as good candidates to study nonlinear optical effects. For example, the observation of the controlled phase shifts up to $\pi/4$ was reported in a single-quantum dot coupled to a photonic crystal nanocavity.¹⁵ In addition, carbon-based systems are promising candidates for spin-based applications^{16–18} because of their long intrinsic decoherence times and zero-spin nuclei.¹⁹ In defect-free CNT QD, it is widely believed that spin-orbit coupling would be weak for both electron and hole, and the electronic states possess electron-hole symmetry.²⁰ Two sets of spin-degenerate orbits are expected to yield a fourfold-degenerate energy spectrum.^{21,22} However, recent theories suggested that the existence of strong spin-orbit coupling in CNTs is due to their curvature and cylindrical topology.²³ More remarkably, Kuemmeth *et al.*,²⁴ by measuring the transport spectroscopy, observed that the interaction between an electron's spin and its orbital motion is strong and the electron-

hole symmetry in such a system is thereby broken down. Based on the strong spin-orbit coupling, it has been pointed out that the spin of electron or hole can be manipulated all optically with high fidelity.²⁵

In our previous work,¹⁰ we studied the tunneling-induced large cross-Kerr nonlinearity in an asymmetric quantum well. However, because the group velocities of the probe and signal fields are mismatched, the nonlinear phase shift cannot be achieved at single-photon level. In the present Brief Report, motivated by these works, we investigate the nonlinear interaction between two ultraweak optical fields in CNT QD with strong spin-orbit coupling based on EIT and demonstrate that a giant cross-Kerr nonlinearity accompanied by suppressed absorptions can indeed be achieved, and yet the probe and signal fields travel with equal propagation velocities utilizing the energy shift produced by strong spin-orbit coupling. Furthermore, we discuss the applications of the proposed scheme in quantum-information processing such as controlled-phase gate operation with high fidelity for two single-photon pulses and generation of entanglement between the signal and probe fields.

We consider a structure [see Fig. 1(a)], in which QD is formed on semiconducting CNT with a diameter $d \sim 1.2$ nm and the lowest optical transition is in the near infrared (~ 1500 nm).²⁶ The topology of CNT separates electron movement into two orbits of equal energy: one that encircles around the nanotube circumference in a clockwise fashion and the other that circles anticlockwise, therefore exhibiting an orbital magnetic moment pointing along the axis.²⁷ In the absence of spin-orbit coupling, the ground states of electron and hole are fourfold degenerate: two of these are orbital states and two are spin states (spin up and spin down). Due to the strong spin-orbit coupling, the zero-field fourfold degeneracy is split into two pairs of doublet states with parallel and antiparallel spin and orbital magnetic moments with energy differences $\Delta_{\text{SO}}^e \approx 1.5$ meV and $\Delta_{\text{SO}}^h \approx 0.9$ meV.^{24,27} The subscript SO and superscript e (h) denote spin-orbit coupling and electron (hole), respectively. The magnetic field couples independently to the spin and orbital moments; therefore the existence of the doublet states

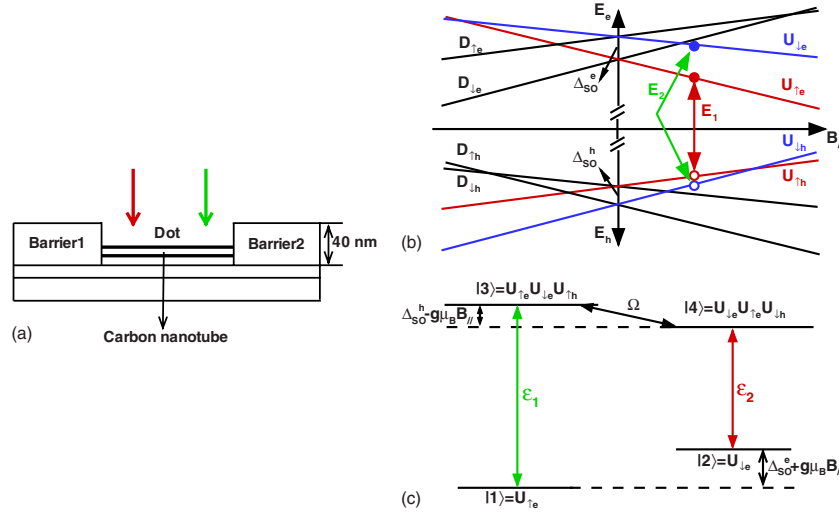


FIG. 1. (Color online) Carbon nanotube quantum dot. (a) Nanotube with two top gates. The probe and signal pulses are applied perpendicular to the CNT axis. (b) Energy diagram of the lowest electron and hole states in a nanotube quantum dot versus the applied axial magnetic field B_{\parallel} . Owing to spin-orbit coupling, the fourfold degeneracy is split into two Kramer doubles: the lower-energy doublet involves states with parallel alignment of orbital and spin magnetic moments, whereas the higher-energy doublet has states with antiparallel alignment. With increasing B_{\parallel} , each state shifts according to its orbital and spin magnetic moments. (c) Equivalent energy diagram of (b) in trion picture. The states $|1\rangle$ and $|2\rangle$ correspond to electrons having parallel and antiparallel alignment of orbital and spin magnetic moments and the states $|3\rangle$ and $|4\rangle$ are formed by exciting one electron from the valence band to conductive band, respectively.

can be revealed by applying a magnetic field B_{\parallel} parallel to the tube axis. It is shown in Fig. 1(b), as a consequence of increasing B_{\parallel} , the spectrum splits into pairs of anticlockwise and clockwise states (going down and up in energy, respectively, i.e., Zeeman splitting).²⁴ The probe and signal fields are, respectively, applied to excite the electron from the valence band to conductive band, yielding two corresponding three-particle states (two electrons and one hole). They are represented by $|3\rangle$ and $|4\rangle$. These two three-particle states couple coherently by the orthogonal component of the magnetic field with strength $\Omega = g\mu_B B_{\perp}/\hbar$. Here, $g \approx 2$ for both electron and hole²⁴ and μ_B is the Bohr magneton. In trion picture, the energy diagram can be described as in Fig. 1(c). In Figs. 1(b) and 1(c), as Imamoğlu and Galland did in Ref. 25, we label the positive- and negative-orbital magnetic moments with U and D , respectively. Due to momentum conservation, only the optical transitions $U \rightarrow U$ and $D \rightarrow D$ are allowed. The up and down arrows denote the projection of the spin along the CNT axis (\uparrow for $S_z = +\hbar/2$) and the subscripts designate electron or hole states.

It is worth noting that the key feature of this structure is that the decay rates from the state $|3\rangle$ to $|2\rangle$ and from $|4\rangle$ to $|1\rangle$ are much smaller than the Rabi frequency Ω and the exciton recombination rates [$\gamma_{31}^{-1} \approx \gamma_{42}^{-1} \approx 40$ ps (Ref. 28)], which is crucial for EIT. As a result, the absorptions of the probe and signal fields are very small and can be ignored when two-photon resonance condition is fulfilled.⁷ In the linear limit, we can view in our qualitative discussion the four-level system [see Fig. 1(c)] as two three-level subsystems, in which both the probe and signal fields exhibit EIT with the same coupling field Ω to induce coherence between two three-particle states. Consequently the widths of their transparency windows could be equal and the probe and signal fields propagate with equal slow group velocities with cer-

tain condition, which is dependent upon spin-orbit coupling. Group-velocity matching is a fundamental condition for achieving a large nonlinear shift because only in this way do the probe and signal fields interact for a sufficiently long time. Upon entering the CNT QD, the probe and signal fields are converted into so-called dark-state polaritons,²⁹ whereby parts of the photonic excitation are temporally transferred to the electron excitation. In order to derive the equations of motion for polaritons, we introduce two new quantum fields $\hat{\Psi}_1$ and $\hat{\Psi}_2$ via the canonical transformations

$$\hat{\Psi}_1(z, t) = \cos \theta_1 \hat{\mathcal{E}}_1(z, t) - \sin \theta_1 \sqrt{N} \hat{\sigma}_{14} / \sigma_{11}^{(0)}, \quad (1a)$$

$$\hat{\Psi}_2(z, t) = \cos \theta_2 \hat{\mathcal{E}}_2(z, t) - \sin \theta_2 \sqrt{N} \hat{\sigma}_{23} / \sigma_{22}^{(0)}, \quad (1b)$$

where N is the number of electrons, $\hat{\mathcal{E}}_{1,2}$ are the corresponding fields operators, $\sigma_{11}^{(0)}$ and $\sigma_{22}^{(0)}$ are the electron distribution in the absence of the probe and signal fields and the mixing angles $\theta_{1,2}$ are defined as

$$\tan \theta_{1,2} = \frac{g_{1,2} \sqrt{N}}{\Omega}. \quad (2)$$

Here $g_1 = \mu_{31} \sqrt{\omega_1 / (2\hbar \epsilon_0 S L)}$ and $g_2 = \mu_{42} \sqrt{\omega_2 / (2\hbar \epsilon_0 S L)}$ are the electron-field coupling constants, with μ_{31} and μ_{42} being the corresponding electron-dipole matrix elements, $\omega_{1,2}$ is the frequencies of the probe and signal fields, S is the cross-section area of the quantum fields, and L is the length of the interaction region. Introducing a plane-wave decomposition of the polariton operators as $\hat{\Psi}_{1,2} = \sum_q \hat{\psi}_{1,2}^q e^{iqz}$, it is easy to check that the mode operators $\hat{\psi}_{1,2}^q$ possess the bosonic commutation relations $[\hat{\psi}_i^q, \hat{\psi}_j^{q'}] = \delta_{ij} \delta_{qq'}$.²⁹ The continuum of modes is bounded by the EIT window and it is scanned by

$q \in \{-\delta q/2, \delta q/2\}$.² By applying adiabatic elimination of the electronic degrees of freedom, one finds the equations of motion for the probe and signal polaritons,

$$\left(\frac{\partial}{\partial t} + \frac{1}{v_1} \frac{\partial}{\partial z}\right) \hat{\Psi}_1(z, t) = -\kappa_1 \hat{\Psi}_1(z, t) + i\eta_1 \hat{\Psi}_1 \hat{I}_2 + \hat{\mathcal{F}}_1, \quad (3a)$$

$$\left(\frac{\partial}{\partial t} + \frac{1}{v_2} \frac{\partial}{\partial z}\right) \hat{\Psi}_2(z, t) = -\kappa_2 \hat{\Psi}_2(z, t) + i\eta_2 \hat{\Psi}_2 \hat{I}_1 + \hat{\mathcal{F}}_2, \quad (3b)$$

where $\hat{I}_{1,2} = \hat{\Psi}_{1,2}^\dagger \hat{\Psi}_{1,2}$ are the intensity operators for the probe and signal polaritons and $\hat{\mathcal{F}}_{1,2}$ the associated δ -correlated noise operators. The group velocities, the single-photon absorption rates, and the cross-Kerr nonlinear interaction terms are, respectively, given by $v_1 = c/(1 + \tan^2 \theta_1 \sigma_{11}^{(0)})$, $v_2 = c/(1 + \tan^2 \theta_2 \sigma_{22}^{(0)})$, $\kappa_1 = -id_{14} \sigma_{11}^{(0)} \tan^2 \theta_1 / c$, $\kappa_2 = -id_{23} \sigma_{22}^{(0)} \tan^2 \theta_2 / c$, $\eta_1 = g_1^2 \sin^2 \theta_2 (\sigma_{22}^{(0)} - \sigma_{11}^{(0)}) / cd_{12}$, and $\eta_2 = g_2^2 \sin^2 \theta_1 (\sigma_{22}^{(0)} - \sigma_{11}^{(0)}) / cd_{12}^*$. Here $d_{14} = \Delta_1 + \delta + i\gamma_{41}$, $d_{23} = \Delta_2 - \delta + i\gamma_{32}$, and $d_{12} = \Delta_1 + \delta - \Delta_2 + i\gamma_{21}$ with single-photon detunings Δ_1 , Δ_2 , and δ , the electron decay rates γ_{41} , γ_{32} , and the spin-flip rate γ_{21} .

For pulsed probe and signal fields, the maximum interaction time could be achieved with group-velocity matching. The expressions of group velocities convey that it is possible to achieve group velocity-matching ($v_1 = v_2 = v$) by preparing suitable electrons in the initial spin states $|1\rangle$ and $|2\rangle$ in such a way that

$$\frac{\sigma_{11}^{(0)}}{\sigma_{22}^{(0)}} = \frac{\tan^2 \theta_2}{\tan^2 \theta_1} = \frac{g_2^2}{g_1^2}. \quad (4)$$

This can be realized with optical spin pumping using resonant laser field.²⁵ Assuming the wave numbers $k_1 \approx k_2 = k$ and $\mu_{31} \approx \mu_{42}$ for simplicity, and recalling the definitions of $g_{1,2}$, then the cross-Kerr nonlinearity terms can be reduced to

$$\eta_1 = g_1^2 \sin^2 \theta_2 (\Delta_{SO}^e + \Delta_{SO}^h) / 2c^2 kd_{12}, \quad (5a)$$

$$\eta_2 = g_2^2 \sin^2 \theta_1 (\Delta_{SO}^e + \Delta_{SO}^h) / 2c^2 kd_{12}^*. \quad (5b)$$

In the absence of spin-orbit coupling, although cross-Kerr nonlinearity can be obtained in such a structure, group-velocity mismatching will prevent the probe and signal fields from interacting for a sufficiently long time. Owing to the energy differences produced by the strong spin-orbit coupling, the combination of giant cross-Kerr nonlinearity and group-velocity matching is not incompatible. Therefore, we can conclude that the giant cross-Kerr nonlinearity in this CNT QD structure is achieved based on both EIT and spin-orbit coupling.

In the semiconducting CNT QD structure under consideration, we note that γ_{41} and γ_{32} are very small. The spin-flip rate, which is dominated by photon-assisted spin relaxation, is expected to have magnitude varying from $1 \mu\text{s}^{-1}$ to 1ms^{-1} . Therefore, if we choose the detunings in such a way that $\Delta_1 = -\Delta_2 = -\delta$ (two-photon resonance) and $\Delta_1 \gg \gamma_{21}$, the single-photon absorption rates are very small and $\eta_{1,2}$ are

purely real. When attenuation and pulse spreading are small enough to be neglected, Eqs. (3a) and (3b) can be easily solved by

$$\hat{\Psi}_1(z, t) = \hat{\Psi}_1(0, \tau) \exp[i\eta_1 \hat{\Psi}_2^\dagger(0, \tau) \hat{\Psi}_2(0, \tau) z], \quad (6a)$$

$$\hat{\Psi}_2(z, t) = \hat{\Psi}_2(0, \tau) \exp[i\eta_2 \hat{\Psi}_1^\dagger(0, \tau) \hat{\Psi}_1(0, \tau) z], \quad (6b)$$

where $\tau = t - z/v$ is the retarded time.

We first consider two single-photon pulses in the classical limit, in which the operators are replaced by their corresponding expectation values. Then the conditional phase shifts accumulated by the probe and signal pulses after their interaction ($t > L/v$) are given by

$$\phi_1 = \phi_2 = \phi \approx \frac{9\pi^2 \gamma_{31}^2 n \lambda^5}{8|\Omega|^2 S} \frac{\Delta_{SO}^e + \Delta_{SO}^h}{\Delta_1}, \quad (7)$$

where $n = N/SL$ is the electron density. In the above derivation, we express the electron-field coupling constant through the corresponding exciton recombination rate and assume $\gamma_{42} = \gamma_{31}$.²⁵ Equation (7) exhibits that the nonlinear phase shift is proportional to the spin-orbit coupling. The lower limit for the coupling Rabi frequency is given by the condition for EIT ($|\Omega|^2 \gg \gamma_{31} \gamma_{41}$), Ω can be chosen to be much smaller than γ_{31} , resulting in the possibility of achieving π phase shift with single photon. For realistic experimental parameters with $T < 10$ K (Ref. 28), $S \approx 1 \mu\text{m}^2$, $N = 1$ (the CNT QD trapping single electron), $L \approx 40$ nm (i.e., the height of QD), $\gamma_{31}^{-1} = 40$ ps, and $\Delta_1 = 0.1$ meV, it can be estimated that the nonlinear phase shift $\phi \approx \pi$ with the fidelity $F \approx 1$ (Ref. 5) can be obtained with $B_\perp \approx 18$ T. Therefore, in a single CNT QD structure, the nonlinear phase shift on the order of π is feasible with single photon because $\phi \propto 1/|\Omega|^2$ [see Eq. (7)]. This is one of the principal results of this Brief Report.

The giant cross-Kerr nonlinearity in such a structure can be applied to semiconducting-based quantum-information processing. Introducing a polarizing beam splitter (PBS), one can realize a transformation corresponding to the controlled-phase logic gate between two traveling single-photon pulses representing qubits. Such a gate has potential capability to build an all-optical quantum computer.³⁰ We therefore investigate the evolution of the two-photon input state $|1\rangle_1 |1\rangle_2$. When $\phi = \pi$, calculations similar to those in Ref. 5 show that the output state of a pair of single photons ($t > L/v$) is given by $|x\rangle_1 |y\rangle_2 = (-1)^{xy} |x\rangle_1 |y\rangle_2$ ($x, y = 0, 1$). Thus, based on EIT and the strong spin-orbit coupling, the controlled-phase gate between the two photons representing qubits is realized.

Next we turn to the fully quantum treatment of the system and investigate the feasibility of generating entanglement of coherent Schrödinger-cat states.⁷ We first analyze the evolution of multimode coherent states $|\Phi_{\text{in}}\rangle = |\alpha_1\rangle \otimes |\alpha_2\rangle$, which is the most ‘‘classical’’ of all the quantum states. The states $|\alpha_j\rangle = \prod_q |\alpha_j^q\rangle$ ($j = 1, 2$) are eigenstates of the input operators $\hat{\Psi}_j(0, t)$ at $z = 0$ with eigenvalues $\alpha_j(t) = \sum_q \alpha_j^q e^{-iqct}$. Upon propagating through the CNT QD, each polariton experiences a nonlinear phase shift. Then the expectation values are obtained as

$$\langle \hat{\Psi}_{1,2}(z, t) \rangle = \alpha_{1,2}(\tau) \exp \left[(e^{i\phi_{1,2}} - 1) \frac{|\alpha_{2,1}(\tau)|^2}{L\delta q} \right], \quad (8)$$

where $\phi_{1,2}$ are the quantum phase shifts. The above solutions have the same forms as those obtained for single-mode³¹ and multimode copropagating fields.^{2,5} Both phases and amplitudes of quantum polaritons exhibit periodic collapses and revivals as $\phi_{1,2}$ change from 0 to 2π . With the absence of spin-orbit coupling, the phases and amplitudes of quantum polaritons remain unchanged (group-velocity matching, no cross-Kerr nonlinear interaction) or separate quickly after a short interaction (group-velocity mismatching). Therefore, the quantum behaviors in such a system are the results of the strong spin-orbit coupling. The time evolution of the input states can also be calculated. It is very interesting that, when $\phi_1 = \pi$, the output state of two fields takes the form

$$|\Phi_{\text{out}}\rangle = \frac{1}{2} (|\alpha_1\rangle \otimes |\alpha_2\rangle + |\alpha_1\rangle \otimes |-\alpha_2\rangle + |-\alpha_1\rangle \otimes |\alpha_2\rangle + |-\alpha_1\rangle \otimes |-\alpha_2\rangle). \quad (9)$$

This is an entangled superposition of macroscopically distinguished states. Such entanglement of coherent Schrödinger-cat states has important applications in scheme of quantum-

information processing and communication with continuous variables.

In summary, we have proposed and studied the highly efficient cross-Kerr nonlinear interaction between two weak optical fields in semiconducting CNT QD structure. By combining electromagnetically induced transparency and the energy differences produced by strong spin-orbit coupling, giant cross-Kerr nonlinearity accompanied by negligible absorption and spectral broadening can be achieved under realistic conditions for CNT QD in which matched group velocities for two interacting pulses can be realized. The attainable π nonlinear phase shift has potential applications in the implementation of high-fidelity controlled-phase gate between two single-photon pulses and generation of entanglement of coherent Schrödinger-cat states. The proposed scheme may therefore pave the way to quantum information such as deterministic all-optical quantum computation based on semiconducting nanomaterials.

We are sincerely grateful to Wei Chen for many fruitful discussions. This work was supported by NUS academic research under Grant No. WBS: R-144-000-189-305. One of the authors (H.S.) would also like to acknowledge the support of the National Basic Research Program of China (973 Program) under Grant No. 2006CB921104 and the author (S.Q.G.) acknowledges funding from the National Natural Science Foundation of China under Grant No. 10874194.

-
- ¹S. E. Harris, J. E. Field, and A. Imamoglu, *Phys. Rev. Lett.* **64**, 1107 (1990).
²M. D. Lukin and A. Imamoglu, *Phys. Rev. Lett.* **84**, 1419 (2000).
³Ying Wu and L. Deng, *Phys. Rev. Lett.* **93**, 143904 (2004); Ying Wu and Xiaoxue Yang, *Appl. Phys. Lett.* **91**, 094104 (2007).
⁴C. Ottaviani, D. Vitali, M. Artoni, F. Cataliotti, and P. Tombesi, *Phys. Rev. Lett.* **90**, 197902 (2003); D. Petrosyan and Y. P. Malakyan, *Phys. Rev. A* **70**, 023822 (2004).
⁵I. Friedler, G. Kurizki, and D. Petrosyan, *Phys. Rev. A* **71**, 023803 (2005).
⁶M. Lukin and A. Imamoglu, *Nature (London)* **413**, 273 (2001).
⁷M. Fleischhauer, A. Imamoglu, and J. P. Marangos, *Rev. Mod. Phys.* **77**, 633 (2005).
⁸H. Schmidt and A. Imamoglu, *Opt. Lett.* **21**, 1936 (1996); **23**, 1007 (1998).
⁹A. Imamoglu, H. Schmidt, G. Woods, and M. Deutsch, *Phys. Rev. Lett.* **79**, 1467 (1997).
¹⁰H. Sun, Y. Niu, R. Li, S. Jin, and S. Gong, *Opt. Lett.* **32**, 2475 (2007).
¹¹Y. F. Chen, C. Y. Wang, S. H. Wang, and Ite A. Yu., *Phys. Rev. Lett.* **96**, 043603 (2006).
¹²S. J. Li, X. D. Yang, X. M. Cao, C. H. Zhang, C. D. Xie, and H. Wang, *Phys. Rev. Lett.* **101**, 073602 (2008).
¹³P. Borri, W. Langbein, S. Schneider, U. Woggon, R. L. Sellin, D. Ouyang, and D. Bimberg, *Phys. Rev. B* **66**, 081306(R) (2002).
¹⁴O. V. Ershova, Yu. E. Lozovik, A. M. Popov, O. N. Bubel, E. F. Kislyakov, N. A. Poklonskii, A. A. Knizhnik, and I. V. Lebedeva, *J. Exp. Theor. Phys.* **107**, 653 (2008).
¹⁵I. Fushman, D. Englund, A. Faraon, N. Stoltz, P. Petroff, and J. Vucković, *Science* **320**, 769 (2008).
¹⁶D. Loss and D. P. DiVincenzo, *Phys. Rev. A* **57**, 120 (1998).
¹⁷N. Mason, M. J. Biercuk, and C. M. Marcus, *Science* **303**, 655 (2004).
¹⁸K. C. Nowack, F. H. L. Koppens, Yu. V. Nazarov, and L. M. K. Vandersypen, *Science* **318**, 1430 (2007).
¹⁹H. W. C. Postma, T. Teepen, Z. Yao, M. Grifoni, and C. Dekker, *Science* **293**, 76 (2001).
²⁰P. Jarillo-Herrero, S. Sapmaz, C. Dekker, L. P. Kouwenhoven, and H. S. J. van der Zant, *Nature (London)* **429**, 389 (2004).
²¹P. Jarillo-Herrero, J. Kong, H. S. J. van der Zant, C. Dekker, L. P. Kouwenhoven, and S. D. Franceschi, *Nature (London)* **434**, 484 (2005).
²²A. Makarovski, A. Zhukov, J. Liu, and G. Finkelstein, *Phys. Rev. B* **75**, 241407(R) (2007).
²³D. Huertas-Hernando, F. Guinea, and A. Brataas, *Phys. Rev. B* **74**, 155426 (2006).
²⁴F. Kuemmeth, S. Ilani, D. C. Ralph, and P. L. McEuen, *Nature (London)* **452**, 448 (2008).
²⁵C. Galland and A. Imamoglu, *Phys. Rev. Lett.* **101**, 157404 (2008).
²⁶R. B. Weisman and S. M. Bachilo, *Nano Lett.* **3**, 1235 (2003).
²⁷E. D. Minot, Y. Yaish, V. Sazonova, and P. L. McEuen, *Nature (London)* **428**, 536 (2004).
²⁸C. Galland, A. Högele, H. E. Türeci, and A. Imamoglu, *Phys. Rev. Lett.* **101**, 067402 (2008).
²⁹M. Fleischhauer and M. D. Lukin, *Phys. Rev. Lett.* **84**, 5094 (2000); *Phys. Rev. A* **65**, 022314 (2002).
³⁰P. Kok, W. J. Munro, K. Nemoto, T. C. Ralph, J. P. Dowling, and G. J. Milburn, *Rev. Mod. Phys.* **79**, 135 (2007).
³¹B. C. Sanders and G. J. Milburn, *Phys. Rev. A* **45**, 1919 (1992).